DR NUBIA BOECHAT (Orcid ID : 0000-0003-0146-2218)

Article type : Research Article

Corresponding author mail id: boechat@far.fiocruz.br

New 1,2,3-triazole-based analogues of benznidazole for use against *Trypanosoma cruzi* infection: *in vitro* and *in vivo* evaluations

Débora Inácio Leite[a,b], Fábio de Vasconcellos Fontes[a,c], Monica Macedo Bastos[a,b], Lucas Villas Boas Hoelz[a], Maria da Conceição Avelino Dias Bianco[a,b], Andressa Paula de Oliveira[a,b,d], Patricia Bernardino da Silva[e], Cristiane França da Silva[e], Denise da Gama Jean Batista[e], Aline Nefertiti Silva da Gama[e], Raiza Brandão Peres[e], Jose Daniel Figueroa Villar[c], Maria de Nazaré Correia Soeiro[e] and Nubia Boechat[a,b*]

[a] *Fundacao Oswaldo Cruz, Instituto de Tecnologia em Farmacos, Farmanguinhos - Fiocruz, Departamento de Sintese de Farmacos, Manguinhos, CEP 21041-250, Rio de Janeiro, RJ, Brazil.*
[b] *Programa de Pos-Graduação em Farmacologia e Quimica Medicinal do Instituto de Ciencias Biomedicas – ICB- UFRJ, Centro de Ciências da Saúde - CCS, Bloco J, Ilha do Fundão, CEP 21941-902 Rio de Janeiro-RJ, Brasil*
[c] *Instituto Militar de Engenharia, Departamento de Ciencia e Tecnologia, Praça General Tiburcio, 80-Praia vermelha, CEP 22290-270, Rio de Janeiro-RJ, Brasil.*
[d] *PROBIN - Abeu - Centro Universitario UNIABEU, Rua Itaiara 301, CEP 26113-400 Belford Roxo-RJ, Brasil.*
[e] *Fundacao Oswaldo Cruz, Instituto Oswaldo Cruz - IOC, Laboratorio de Biologia Celular, Manguinhos, CEP 21040-900, Rio de Janeiro, RJ, Brazil.*

Short running title: New 1,2,3-triazoles analogues of benznidazole

Keywords: Benznidazole; 2-nitroimidazole; 1,2,3-triazoles; click chemistry

ABSTRACT

Chagas disease (CD) has spread throughout the world mainly because of the migration of infected individuals. In Brazil, only benznidazole (Bnz) is used; however, it is toxic and not active in the chronic phase, and cases of resistance are described. This work aimed at the synthesis and the trypanocidal evaluation *in vitro* and *in vivo* of six new Bnz analogues (**3-8**). They were designed by exploring the bioisosteric substitution between the amide group contained in Bnz and the 1,2,3-triazole ring. All the compounds were synthesized in good yields. With the exception of compound **7**, the *in vitro* biological evaluation shows that all Bnz analogues were active against the amastigote form, whereas only compounds **3**, **4**, **5**, and **8** were active against trypomastigote. Compounds **4** and **5** showed the most promising activities *in vitro* against the form of trypomastigote, being more active than Bnz. *In vivo* evaluation of compounds, **3-8** showed lower potency and higher toxicity than Bnz. Although the 1,2,3-triazole ring has been described in the literature as an amide bioisostere, its substitution here has reduced the activity of the compounds and made them more toxic. Thus, further molecular optimization could provide novel therapeutic agents for Chagas' disease.

1. Introduction

In the last two decades, the migration patterns of people from South and Central America to North America, Asia, and Europe have changed the outlook of Chagas disease (CD), an illness caused by infection of the protozoan parasite *Trypanosoma cruzi* (*T. cruzi*). The number of infected people worldwide is higher than 6 million, with 300 thousand to 1 million estimated in the United States, 24 to 38 thousand in Europe, and 12 to 25 thousand in Spain alone.[1–3] CD is also endemic in Latin America, killing more than 15,000 people each year. In Brazil, there are approximately 2 to 3

million patients with chronic CD and more than 6,000 annual deaths, and CD-related spending accounts for $129 million of the public budget.[4,5] Additionally, current reports demonstrate that the annual global CD-related healthcare costs are approximately $627 million, of which $118 million is spent in the United States.[6]

The available drugs for the treatment of CD, benznidazole (**1**, Bnz) and nifurtimox (**2**), emerged in the late 1960s and early 1970s[7] (Figure 1). However, in Brazil, only Bnz is used for treatment.

Although many works report Bnz as an inducer of the formation of free radicals and electrophilic metabolites within *T. cruzi*, when its nitro moiety is reduced to an amino group by the action of nitroreductases, its exact mechanisms of action are still unclear.[8–10] Moreover, Rajão and co-workers describe that Bnz preferentially oxidizes the nucleotide pool, and the extensive incorporation of oxidized nucleotides, during DNA replication, leads to potentially lethal double-stranded DNA breakage, preventing parasite multiplication.[10] Clinical treatment with Bnz is long, lasting up to 90 days (with doses of 5 to 7 mg/kg/day), and the treatment cures 60 to 80% of patients in the acute phase.[11] However, in the chronic phase of the disease, approximately ≥ 80% of the treated patients are not cured.[12] In addition to being genotoxic, this drug can also cause muscle pain, joint pain, paraesthesia, cutaneous hypersensitivity with the appearance of rash, generalized oedema, thrombocytopenia, fever, lymphadenopathy, purpura and agranulocytosis, peripheral neuropathy and polyneuropathy.[12] In addition, Bnz is ineffective in treating some naturally resistant strains, which is concerning to healthcare organizations.[13] Therefore, the search for new analogues of this drug could be important in the treatment of the CD.

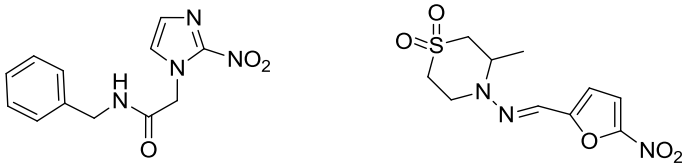

Benznidazole **(1)** Nifurtimox **(2)**

Figure 1. Chemical structures of benznidazole (**1**, Bnz) and nifurtimox (**2**), which are used in the treatment of Chagas disease.

In medicinal chemistry, 1,2,3-triazole groups are utilized as linkers between two or more pharmacophoric groups and are described as bioisosteres of amide groups owing to their similar physicochemical properties.[14,15] This strategy, known as molecular hybridization, has been applied in the identification of new and unique structural patterns that may represent new candidates and prototypes compounds with new pharmacological profiles and properties;[16,17] for example, these compounds could present higher lipophilicity and stability.[14,15] Thus, 1,2,3-triazole rings are broadly applicable and can be used in compounds such as antiparasitic,[16,18,19] anticarcinogenic,[20,21] antiviral,[22,23] bactericidal,[24–26] antiepileptic,[27] enzyme inhibiting[28,29] and sleep regulating[30] compounds. The literature also describes other applications for these compounds, for example, in explosives[31,32] and agrochemicals.[33] The 1,2,3-triazole 1,4-disubstituted rings are easy to obtain using "click chemistry" and, since click chemistry was conceived, it has had a great impact in many areas of modern chemistry.[34] In 2015, some 1,2,3-triazole analogues of benznidazole were described[35] by Carvalho and co-workers, that kept *N*-benzyl-acetamide scaffold and the bioisosteric replacement of 1*H*-imidazole moiety by a 1,2,3-triazole ring was explored. The results showed that most compounds were less active than benznidazole.[35]

Therefore, in the present work, we report six new analogues of Bnz (**3**-**8**), including their design, synthesis and biological evaluation. All these compounds contain a 1,2,3-triazole ring in their structure, and the substitution of the amide functional group with a 1,2,3-triazole ring could be justified because they present similar physicochemical properties, volume and planarity.[36,37] In compound **3**, the moiety of Bnz was maintained in the structure, replacing only the amide group by a 1,2,3-triazole ring, making compound **3** an isostere of Bnz. For compounds **4** and **5**, the benzyl group of Bnz was replaced by a phenyl ring containing different substituents with the aim of studying the effect of the substituents and the methylene spacer between the aromatic ring and 1,2,3-triazole on the antichagasic activity (Scheme 1). In compound **6**, a phenylamide group was used to verify the importance of introducing an additional amide group in the structure. The proposed derivatives **7**-**8** were designed using the concepts of molecular hybridization. A phosphonate group was added to compound **7**, a moiety present in risedronate (**9**), which is active *in vitro* and *in vivo* against the parasite *T. cruzi*.[38,39] The second pharmacophoric fragment used in compound **8** was 7-chloroquinoline, which has known antichagasic activity,[40] as can be seen in compound **10**, also used as a prototype (Scheme 1).

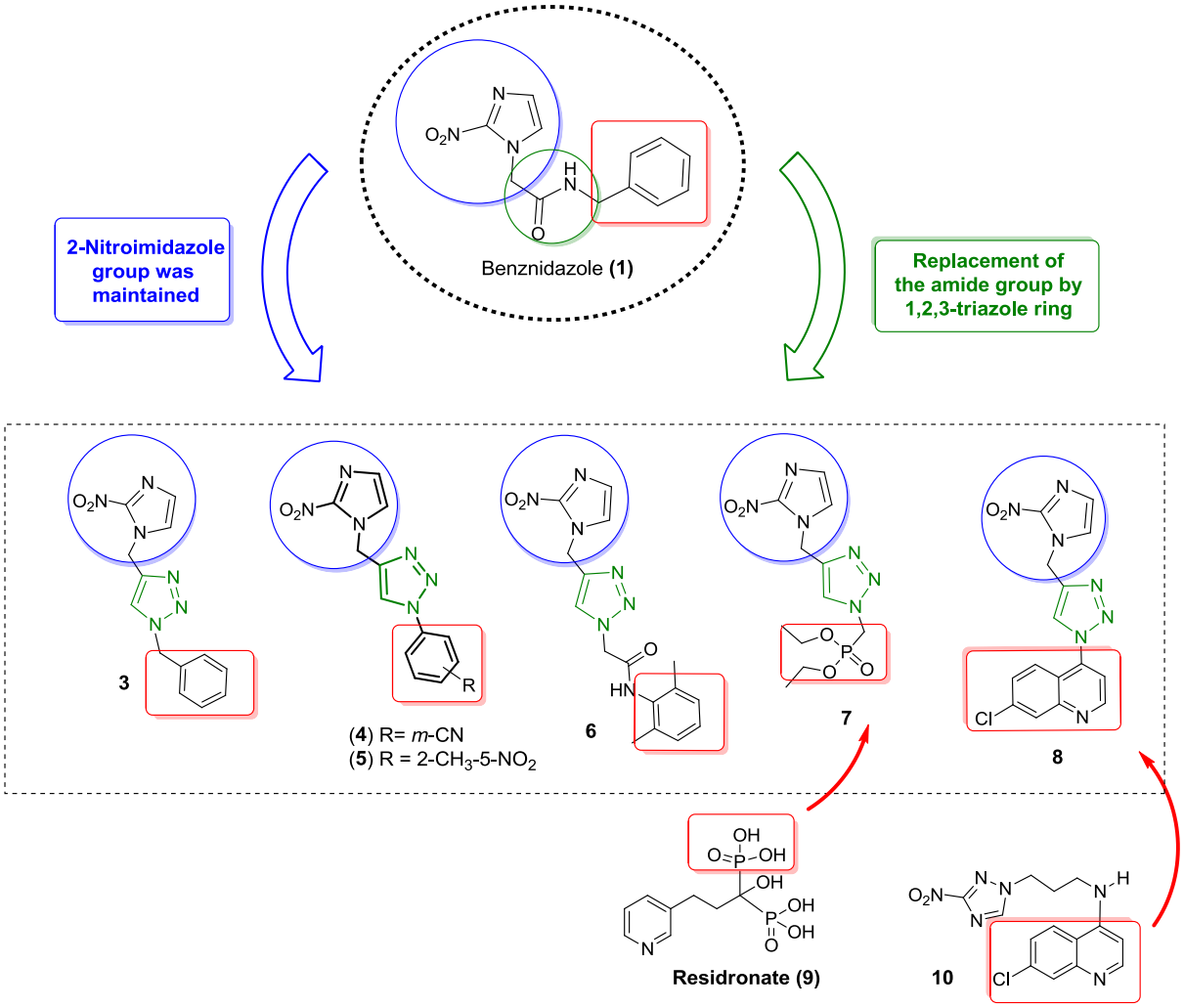

Scheme 1. Design of new derivatives **3-8**.

2. Methods and Materials

2.1. Chemistry

Melting points were determined in Büchi B-545 apparatus, and the values were not corrected. Reactions were monitored by thin layer chromatography (TLC) using aluminium-supported silica gel cromatoplates with an indicator, and spots were visualized with ultraviolet (UV) light (254 and 366 nm). Gas chromatography coupled to electron impact mass spectrometry (GC-MS) was conducted at 70 eV on an HP 6890 apparatus using a DB-5 phase column (30 m long, 0.25 µm film thickness, 0.25 mm internal diameter). The carrier gas was helium flowing at 0.5 mL/min and the split was 10: 1. Analysis conditions included an initial column temperature of 50 °C, a gradient of 10 °C/min, a final column temperature of 300 °C column, an injector temperature of 270 °C, and in interface temperature of 280 °C. Low-resolution mass spectra were acquired by electrospray ionisation mass spectrometry (MS-ESI). The molecular ion was described in terms of atomic mass units and the ratio thereof (*m/z*), and the relative abundance was expressed as a percentage. Infrared spectra were acquired on a Thermo Scientific spectrophotometer, Nicolet 6700 model. The values of the absorptions are reported in wavenumbers in inverse centimetres (cm^{-1}). Nuclear magnetic resonance (NMR) spectra were obtained at 400 and 600 MHz for hydrogen, 100 and 150 MHz for carbon and 400 MHz for phosphorus. Trimethylsilane (TMS) was used as internal reference standard for hydrogen and carbon (0 ppm). Chemical shifts were reported in dimensionless units (δ) representing parts per million (ppm). The relative areas of the signals were obtained by electronic integration, and their multiplicities are described as singlet (s), doublet (d), triplet (t), multiplet (m), doublet of doublets (dd) or doublet of triplets (dt). High-resolution mass

spectra (HRMS) were acquired using a mass spectrometer with electron ionization (MS-ESI, digitalizing ES+capilar). Analytical HPLC analyses were conducted with a LaChrom system (Merck Hitachi). The eluent was monitored from 190-800 nm. The flow of the mobile phases of all analyses was 0.7-1.0 mL/min, and the injected volume was 10 µL. Separation was obtained on a Supelcosil column LC-18 4.6 x 150 mm (particle diameter of 3 µm) and a Supelguard LC-18 (2 cm) pre-column.

2.1.1. Preparation of 2-nitro-1-(prop-2-yn-1-yl)-1H-imidazole (11)

The synthesis of 2-nitro-1-(prop-2-yn-1-yl)-1*H*-imidazole (**11**) was described in the literature.[41–43] In this work, a mixture of 2-nitroimidazole (**18**) (0.0088 mol, 1 g), anhydrous potassium carbonate (1.9 mol, 2.32 g), sodium iodide (0.32 mol, 0.42 g), 3-bromoprop-1-yne (1.6 mol, 1.70 g) and 18-crown-6 (0.0088 mol, 0.094 g) in DMF anhydrous (30 mL) were combined and stirred at room temperature for 1 h. To isolate the product, the reaction mixture was vacuum filtered and washed with 10 mL of DMF. Then, the filtrate was evaporated, and the product was extracted with ethyl acetate (6 x 25 mL) and washed with water. The organic phase was dried with anhydrous Na_2SO_4, and the solvent was removed by evaporation. The product was obtained as a yellow oil. Yield: 86%. IR (ATR, cm^{-1}): 3287 (C-H alkyne), 2133 (C≡C), 1537, 1355 (NO_2), 1482 (C=N). ^{1}H NMR (600 MHz, DMSO-d_6, ppm) δ: 3.61 (t; *J*= 3.0 Hz, 1H, C≡C-H); 5.28 (d; *J*= 2.4 Hz, 2H, CH_2); 7.21 (d, *J*= 1.0 Hz, 1H, C-4 Ar-H); 7.76 (d, *J*= 1.0 Hz, 1H, C-5 Ar-H). ^{13}C NMR (150 MHz, DMSO-d_6, ppm) δ: 39.22 (CH_2); 77.16 (C≡C-H); 77.27 (C≡CH); 127.03 (C-2 Ar); 127.86 (C-3 Ar); 144.15 (C-NO_2). GC-MS (70 eV, *m/z*, %): 151 (100), 106 (44), 97 (55), 93 (55), 79 (34).

2.1.2. General procedure for the synthesis of azides 12-17

Azides **12**, **15** and **16** were prepared according to the methodologies previously described in the literature.[15,44–46]

The methodologies described by Boechat and co-workers were used for the syntheses of azides **13**, **14** and **17**.[15,18]

2.1.3. General procedure for the synthesis of final products 3-8

The literature described many methodologies for the synthesis of 1,2,3-triazole ring, using the 2-nitro-1-(prop-2-yn-1-yl)-1*H*-imidazole (**11**) as starting materials.[41–43,47] In this work, these compounds were prepared through the reaction of azides **12-17** (2.2 mmol) and 2-nitro-1-(prop-2-yn-1-yl)-1*H*-imidazole (**11**) (2.8 mmol), sodium ascorbate (0.22 mmol), copper sulfate (0.13 mmol) and 20 mL of a mixture of *t*-butanol: water (1: 1). The reaction was kept under magnetic stirring at room temperature for 6-30 h. The completion of reaction was determined by TLC using ethyl acetate: hexane (4: 6) as the eluting system. The mixture was diluted with 20 mL of water, and then the product was extracted with ethyl acetate (6 x 25 mL). The organic phase was dried with anhydrous Na_2SO_4, and the solvent was removed by evaporation. All products were purified by column chromatography using chloroform: methanol (9.5: 0.5).

2.1.3.1. 1-Benzyl-4-((2-nitro-1H-imidazol-1-yl)methyl)-1H-1,2,3-triazole (3)

Reaction time: 6 h. Yield: 69%. Yellow solid. m.p.: 129-131 °C. IR (ATR, cm^{-1}): 3137 (C-H sp^2); 1532 e 1357 (N=O); 1481 (C=N); 760; 739; 709 (C-H Ar). ^{1}H NMR (400 MHz, Acetone-d_6, ppm) δ: 5.63 (s, 2H, CH_2-N1'); 5.77 (s, 2H, CH_2-N1''); 7.11 (d, *J*= 0.96 Hz, 1H, H-4''); 7.33-7.37 (m, 5H, H-Ar); 7.57 (d, *J*= 0.96 Hz, 1H, H-5''); 8.06 (s, 1H, H-5'). ^{13}C NMR (100 MHz, Acetone-d_6, ppm) δ: 45.51 (CH_2-N1''); 54.30 (CH_2-N1'); 124.29 (C-5'); 127.84 (C-5''); 127.96 (C-2); 128.66 (C-4''); 128.93 (C-4); 129.17 (C-3); 129.70 (C-1); 136.80 (C-4'); 143.06 (C-2''). MS-ESI [$(M)^+$, %): 284.4 (100). HRMS: calculated for: 284.1022, found: 284.1023. HPLC (320 nm): 97.0%.

2.1.3.2. 3-((4-((2-Nitro-1H-imidazole-1-yl)methyl)-1H-1,2,3-triazole-1-yl)methyl)benzonitrile (4)

Reaction time: 20 h. Yield: 60%. Orange solid. m.p.: 184-186 °C. IR (ATR, cm^{-1}): 3090 (C-H sp^2); 1530 and 1356 (N=O); 2232 (C≡N). ^{1}H NMR (600 MHz, DMSO-d_6, ppm) δ: 5.82 (s, 2H, CH_2-N1''); 7.25 (d, *J*= 4.6 Hz, 1H, H-4''); 7.79 (d, *J*= 7.8 Hz, 1H, H-5); 7.81 (d, *J*= 4.6 Hz, 1H, H-5''); 7.96 (dt, *J*= 1.1 Hz; 7.8 Hz, 1H, H-4); 8.28 (dd, *J*= 3.0

Hz; 8.4 Hz, 1H, H-6); 8.43 (t, *J*= 2.3 Hz, 1H, H-2); 8.90 (s, 1H, H-5'). ^{13}C NMR (150 MHz, DMSO-d_6, ppm) δ: 44.53 (CH_2-N1"); 112.72 (C-3); 117.74 (CN); 122.14 (C-5'); 124.73 (C-6); 125.52 (C-2); 127.98 (C-5"); 128.01 (C-4"); 131.24 (C-5); 132.26 (C-4); 136.84 (C-1); 143.40 (C-4'); 144.44 (C-2"). MS-ESI [$(M-1)^+$, %): 308.0 (100). HRMS: calculated for: 309.0974, found: 309.0978. HPLC (320 nm): 98.4%.

2.1.3.3. 1-(2-Methyl-5-nitrophenyl)-4-((2-nitro-1H-imidazole-1-yl)methyl)-1H-1,2,3-triazole (5)

Reaction time: 28 h. Yield: 67%. Yellow solid. m.p.: 149-151 °C. IR (ATR, cm^{-1}): 3142 (C-H sp^2); 1521 and 1344 / 1503 and 1344 (N=O); 1481 (C=N). ^{1}H NMR (600 MHz, DMSO-d_6, ppm) δ: 2.28 (s, 3H, CH_3-Ar); 5.83 (s, 2H, CH_2-N1"); 7.24 (d, *J*= 4.6 Hz, 1H, H-4"); 7.78 (d, *J*= 8.2 Hz, 1H, H-3); 7.80 (d, *J*= 4.6 Hz, 1H, H-5"); 8.33 (s, 1H, H-6); 8.34 (d, *J*= 8.2 Hz, 1H, H-4); 8.65 (s, 1H, H-5'). ^{13}C NMR (150 MHz, DMSO-d_6, ppm) δ: 17.88 (CH_3Ar); 44.34 (CH_2-N1"); 121.19 (C-6); 124.37 (C-4); 125.78 (C-5'); 127.90 (C-4"); 127.91 (C-5"); 132.74 (C-3); 136.33 (C-1); 141.46 (C-2); 141.99 (C-4'); 144.50 (C-2); 146.06 (C-5). MS-ESI ([M-1]$^+$, %): 328.1 (100). HRMS: calculated for: 329.0873, found: 329.0871. HPLC (320 nm): 99.0%.

2.1.3.4. N-(2,6-Dimethylphenyl)-2-(4-((2-nitro-1H-imidazole-1-yl)methyl)-1H-1,2,3-triazole-1-yl)acetamide (6)

Reaction time: 18 h. Yield: 65%. White solid. m.p.: 175 °C (degradation). IR (ATR, cm^{-1}): 3243 (N-H); 3142 (C-H sp^2); 1665 (C=O); 1530 and 1356 (N=O); 1478 (C=N). ^{1}H NMR (400 MHz, DMSO-d_6, ppm) δ: 2.13 (s, 6H, CH_3-Ar); 5.35 (s, 2H, CH_2-N1'); 5.73 (s, 2H, CH_2N1"); 7.06-7.08 (m, 3H, H-3, H-4, H-5); 7.20 (d, *J*= 0.92 Hz, 1H, H-4"); 7.73 (d, *J*= 0.92 Hz, 1H, H-5"); 8.17 (s, 1H, H-5'); 9.73 (s, 1H, N-H). ^{13}C NMR (100 MHz, DMSO-d_6, ppm) δ:17.86 (CH_3-Ar); 44.33 (CH_2-N1"); 51.59 (CH_2N1'); 125.22 (C-5'); 126.66 (C-4); 127.64 (C-3); 127.74 (C-5"); 127.81 (C-4"); 134.03 (C-2); 134.97 (C-1); 141.28 (C-4'); 144.27 (C-2"); 163.82 (C=O). MS-ESI ([M-1]$^+$, %): 354.2 (100). HRMS: calculated for: 355.1393, found: 355.1377. HPLC (320 nm): 99.2%.

2.1.3.5. Diethyl ((4-((2-nitro-1H-imidazole-1-yl)methyl)-1H-1,2,3-triazole-1-yl)methyl)phosphonate (7)

Reaction time: 23 h. Yield: 62%. Yellow oil. IR (ATR, cm^{-1}): 3137 (C-H sp^2); 1537 and 1366 (N=O); 1488 (C=N); 1246 (P=O); 1013 (C-O). ^{1}H NMR (400 MHz, Acetone-d_6, ppm) δ: 1.23 (t, *J*= 14 Hz, 6H, CH_3); 4.06-4.13 (m, 4H, CH_2-O); 4.97 (d, *J*= 14 Hz, 2H, CH_2-N1); 5.81 (s, 2H, CH_2N1'); 7.13 (d, *J*= 1.0, 1H, H-4'); 7.60 (d, *J*= 1.0, 1H, H-5'); 8.08 (s, 1H, H-5). ^{13}C NMR (100 MHz, Acetone-d_6, ppm) δ: 16.59 (CH_3); 45.43 (CH_2N-1'); 46.93 (CH_2N-1); 63.64 (CH_2-O); 125.33 (C-5); 127.89 (C-5'); 128.69 (C-4); 142.97 (C-2'). ^{31}P NMR (400 MHz, DMSO-d_6, ppm) δ: 16.19. MS-ESI [$(M+Na)^+$, %]: 367.0 (100). HRMS: calculated for: 344.0998, found: 344.0999. HPLC (320 nm): 99.9%.

2.1.3.6. 7-Chloro-4-(4-((2-nitro-1H-imidazole-1-yl)methyl)-1H-1,2,3-triazole-1-yl)quinoline (8)

Reaction time: 30 h. Yield: 51%. Yellow solid. IR (ATR, cm^{-1}): 3137 (C-H sp^2); 1537 and 1366 (N=O); 1488 (C=N); 823; 795; 738 (CH-Ar). ^{1}H NMR (600 MHz, DMSO-d_6, ppm) δ: 5.89 (s, 2H, CH_2-N1"); 7.26 (d, *J*= 4.6 Hz, 1H, H-4"); 7.78 (dd, *J*= 9.0 Hz; 2.0 Hz, 1H, H-6); 7.84 (d, *J*= 4.6, 1H, H-3); 7.85 (d, *J*= 4.6, 1H, H-5"); 7.98 (d, *J*= 9.0, 1H, H-5); 8.27 (d, *J*= 2.0 Hz, 1H, H-8); 8.87 (s, 1H, H-5'); 9.14 (d, *J*= 4.6 Hz, 1H, H-2). ^{13}C NMR (150 MHz, DMSO-d_6, ppm) δ: 44.33 (CH_2-N-1"); 117.20 (C-3); 120.28 (C-4a); 125.40 (C-5); 126.10 (C-5'); 127.98 (C-4'); 128.00 (C-5"); 128.12 (C-8); 128.93 (C-4"); 135.37 (C-7); 140.21 (C-4); 142.60 (C-4'); 144.55 (C-2"); 149.35 (C-8a); 152.32 (C-2). MS-ESI [$(M+Na)^+$, %]: 378.1 (100). HRMS: calculated for: 355.0585, found: 355.0585. HPLC (320 nm): 98.9%.

2.2 Biological evaluation

2.2.1 Compounds

The stock solutions for the *in vitro* and *in vivo* analysis of the compounds against *T. cruzi* were prepared in dimethyl sulfoxide (DMSO) with the final concentration of the solvent never exceeding 0.6% and 10%, respectively, which was not toxic (data are not shown). Benznidazole (Bnz) (2-nitroimidazole; Laboratório Farmacêutico do Estado de Pernambuco [LAFEPE], Brazil) was used as the reference drug, and aliquots were stored at -20 °C.

2.2.2. Mammalian cell cultures

For the *in vitro* analysis of compound toxicity and effect against intracellular forms of *T. cruzi* (Tulahuen strain expressing the *Escherichia coli* β-galactosidase gene), monolayers of mouse L929 fibroblasts were cultivated (4 x 10^3 cell/well into 96-well microplates) at 37 °C in RPMI-1640 medium (pH 7.2-7.4) without phenol red (Gibco BRL) supplemented with 10% foetal bovine serum (FBS) and 2 mM glutamine (RPMIS), as reported.[48,49]

2.2.3. Parasites and infection of the cell cultures

Tissue culture-derived trypomastigotes (Tulahuen strain expressing the *E. coli* β-galactosidase gene) were maintained in L929 cell lines and collected from the supernatants after 96 h of parasite infection following previously established protocols.[48] Briefly, 24 h after L929 platting (4 x 10^3 cells/well), the cultures were incubated with trypomastigotes (using a 10:1 ratio) for 24 h at 37 °C. Then, the cell cultures were rinsed to remove non-internalized parasites and then further incubated for another 24 h at 37 °C. Bloodstream trypomastigote (BT) forms of the Y strain of *T. cruzi* were obtained from the blood of infected male Swiss mice at the peak of parasitaemia.[50] The purified parasites were resuspended in RPMI-1640 medium (pH 7.2-7.4) without phenol red (Gibco BRL) supplemented with 10% foetal bovine serum (FBS) and 2 mM glutamine (RPMIS), as reported previously.[49]

2.2.4. Cytotoxicity assay

L929 cell cultures were incubated for 96 h at 37 °C with different concentrations of each compound (up to 200 µM) diluted in DMEM (without phenol red). The morphology and spontaneous contractibility of the cells were evaluated by light microscopy, and then their cellular viability was determined by the alamarBlue® assay. For this colourimetric bioassay, 10 µL of alamarBlue® (Invitrogen) was added to each well, and the plate was incubated for an additional 24 h, after which the absorbances at 570 and 600 nm were measured. As negative controls, alamarBlue® assays were also performed without cells, running only DMEM and DMEM containing each tested compound (at higher concentrations). The results were expressed as percent difference in reduction between compound treated and vehicle treated cells following the manufacturer's instructions, and the EC_{50} values correspond to the concentrations required to reduce cellular viability by 50%.[51]

2.2.5. Trypanocidal analysis

BT forms of the Y strain (5 x 10^6 per mL) were incubated for up to 24 hours at 37 °C in RPMI in the presence or absence of serial dilutions of the compounds (0 to 50 µM). After compound incubation, the parasite death rates were determined by light microscopy through the direct quantification of the number of live parasites using a Neubauer chamber, and the EC_{50} values (concentration that reduces the number of parasites by 50%) for each compound were calculated.[49] For the assay on intracellular forms, the Tulahuen strain was employed using L929 cells. Briefly, Tulahuen-infected L929 cultures were exposed to 10 µM (corresponding to the EC_{90} value of Bnz, as reported by Romanha and co-workers)[48] of each compound diluted in RPMIS, and those compounds that caused ≥ 50% reduction in the parasite infection were further screened under increasing concentrations aiming to determine the EC_{50} values.[49] After 96 h of incubation with the test compounds at 37 °C, chlorophenol red glycoside (500 µM) in 0.5% Nonidet P40 was added to each well and the plate was incubated for another 18 h at 37 °C. Then, the absorbance was measured at 570 nm. Uninfected and *T. cruzi*-infected cultures treated with the vehicle and Bnz were run in parallel. The results are expressed as the percentage of *T. cruzi* growth inhibition in compound-tested cells compared to the infected cells and untreated cells.[48] Triplicate samples were run on the same plate, and at least two assays were performed in duplicate for each analysis.

2.2.6. In vivo infection

Swiss Webster male mice (18-20 g) obtained from the animal facilities of CECAL were housed at a maximum of 6 per cage and kept in a specific pathogen free (SPF) room at 20–24 °C under a 12/12 h light/dark cycle and provided with sterilized water and chow ad libitum. The animals were allowed to acclimate for 7 days before starting the experiments. Infection was performed by intraperitoneal (ip) injection of 10^4 bloodstream trypomastigotes (Y strain). Age-matched non-infected mice were maintained under identical conditions.[50]

2.2.7. Treatment schemes

Compounds were first dissolved in DMSO and then freshly diluted with sterile distilled water. The stock solution of benznidazole (*N*-benzyl-2-nitroimidazole acetamide) was prepared in sterile distilled water with 3% Tween 20. The animals were divided into the following groups: uninfected (non-infected and non-treated); untreated (infected but treated only with vehicle); and treated (infected and treated with the compounds). The mice therapy was performed through different schemes. First, *T. cruzi*-infected mice were treated with 25 mg/kg/day (via ip injection) and 100 mg/kg/day Bnz (by p.o.) at 5 and 8 dpi, which correspond to the onset and peak of the parasitaemia using Y strain in this experimental model, respectively. Next, mice infected with *T. cruzi* were treated for 5 consecutive days starting at the onset of parasitaemia (at 5 dpi, which corresponds to the onset of parasitaemia using this naturally mild resistant strain in this experimental model) with up to 100 mg/kg/day for the tested compound or 100 mg/kg for Bnz). In all assays, only mice with positive parasitaemia were used in the infected groups.

2.2.8. Parasitaemia and mortality rates

Parasitaemia was individually determined by direct microscopic counting of parasites in 5 µL of blood, and mortality rates were determined daily until 30 days post-treatment and expressed as a percentage of cumulative mortality (% CM) as described before.[49]

2.2.9. Ethics

All procedures were carried out in accordance with the guidelines established by the FIOCRUZ Committee of Ethics for the Use of Animals (CEUA LW16/14).

3. Results and Discussion

3.1. Chemistry

The final compounds **3-8** were prepared using "click chemistry" with terminal acetylene 2-nitro-1-(prop-2-en-1-yl)-1*H*-imidazole (**11**), a key intermediate in obtaining the planned compounds, and the appropriate azides (**12-17**). The azides were synthesized through one of two methodologies: either *via* bimolecular nucleophilic substitution or *via* nucleophilic aromatic substitution[15,18,52,53] (Scheme 2).

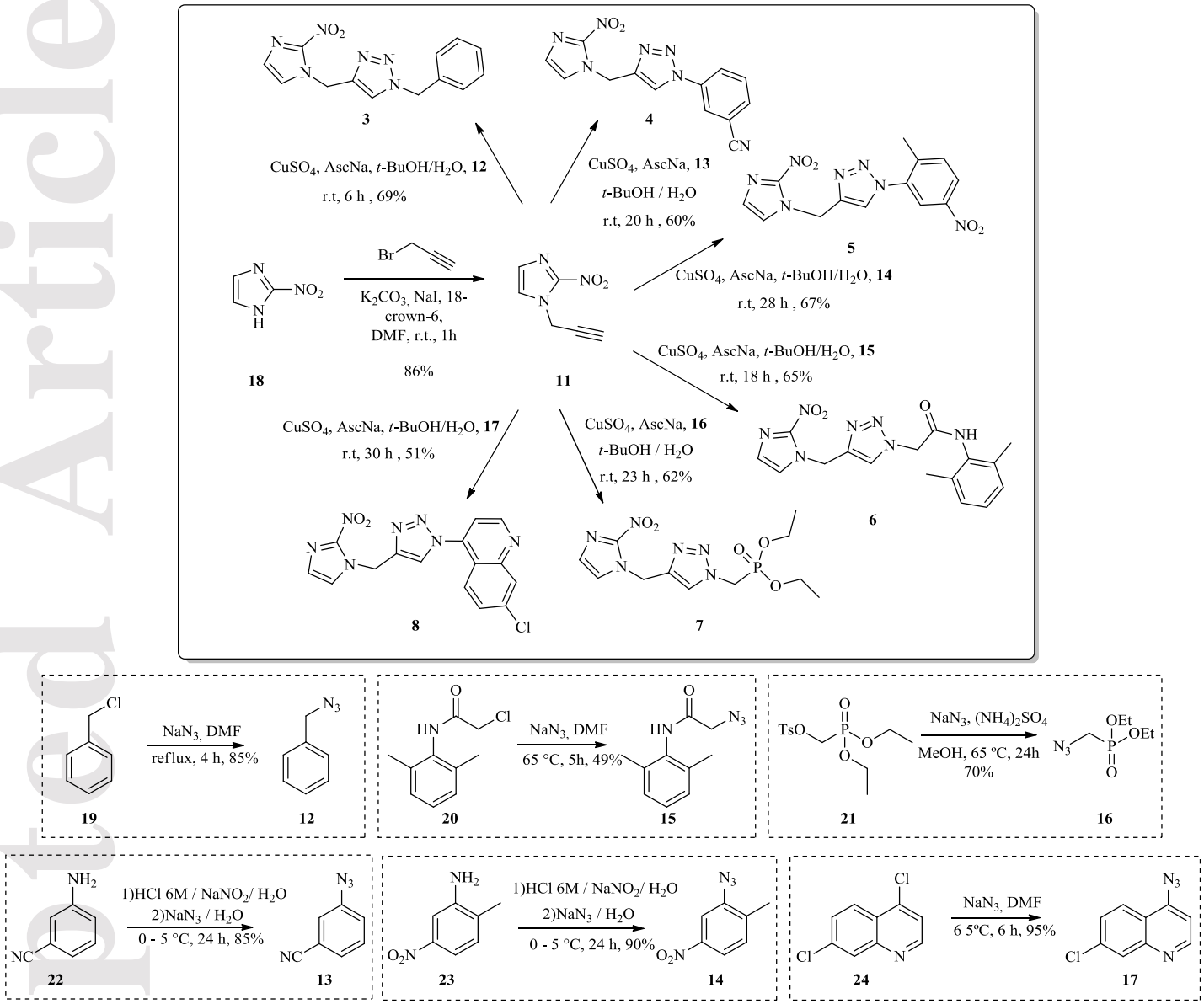

Scheme 2. Synthetic methodology for the preparation of final products **3-8**.

3.1.1. Synthesis of key intermediate (11)

The synthesis of 2-nitro-1-(prop-2-yn-1-yl)-1*H*-imidazole (**11**), described by Joyard and co-workers, occurs through the alkylation of 2-nitroimidazole (**18**) *via* bimolecular nucleophilic substitution using propargyl iodide generated *in situ* from propargyl bromide.[43] 18-Crown-6 was used as a phase transfer catalyst, and potassium carbonate was used as the base in dimethylformamide (DMF) at room temperature for one hour (Scheme 2). Intermediate **11** was obtained as a yellow oil in 86% yield, and its chemical structure was confirmed by liquid chromatography-mass spectrometry (LC-MS) and infrared (IR) and ^{1}H and ^{13}C nuclear magnetic resonance (NMR) spectroscopies. The results of the analyses were compared with the literature data since this intermediate are already described.[41–43]

3.1.2. Synthesis of azides (12-17)

Although organic azides can be explosive and toxic, they are very attractive reagents for the pharmaceutical industry. In this paper, azides **12**, **15** and **16** were synthesized *via* nucleophilic bimolecular substitution through nucleophilic attack by azide anion on the leaving group; the reactions required heating, and reaction times varied from 4-24 hours.[45,46] Yields of the azides varied between 49 and 85% (Scheme 2), and the chemical structures were confirmed by mass spectrometry with electrospray ionisation mass spectrometry (MS-ESI) and IR. The results of the analyses were compared with the literature data since these intermediates are already described.[15,44–46]

Azides **13**, **14** and **17** were obtained by nucleophilic aromatic substitution, and **13** and **14** were prepared from the diazonium salt. In those cases, the first step was the formation of the electrophile (nitronium ion), which is then attacked by the lone pair of electrons of the aromatic amine, forming the salt. Subsequently, azide anion is added the intermediate, generating products **13** and **14** in 85% and 90% yield, respectively[18] (Scheme 2). 4-Azido-7-chloroquinoline (**17**) was synthesized by the reaction between 4,7-dichloroquinoline (**24**) and NaN_3 in DMF at 65 °C for 6 hours[15] (Scheme 2). **17** was obtained as a white solid in 95% yield. Chemical structures of the azides were confirmed by MS-ESI and IR. The results of the analyses were compared with the literature data since these intermediates are already described.[15,18]

3.1.3. Synthesis of final products 3-8

All final compounds have a 1,2,3-triazole ring in their structure. This ring was obtained through a 1,3-dipolar cycloaddition reaction involving a dipolarophile; in this case, the dipolarophile was a terminal alkyne with a 1,3-dipolar molecule, the azido group, which generates a five-membered heterocycle. Thus, the key intermediate, acetylene **11**, was reacted with the synthesized azides **12-17** using "click chemistry" (Scheme 2).

Final products **3-8** were purified by column chromatography to remove excess acetylene, and the desired products were obtained in 51-69% yields. The chemical structures were confirmed by MS-ESI, IR, high-resolution mass spectrometry (HRMS), and ^{1}H, ^{13}C, and ^{31}P NMR.

The absorption band corresponding to axial deformation of the N=N bond, characteristic of azides, was not present in the IR spectra of final products **3-8**. Characteristic absorptions were observed between 1521 and 1344 cm^{-1}, corresponding to axial deformation of the connecting N=O. In product **5**, absorptions between 1521 and 1344 cm^{-1} were observed in duplicate, and these bands correspond to the axial deformation of the connecting N=O. For compound **7** absorptions between 1246 and 1239 cm^{-1} were observed, corresponding to the axial deformation of the P=O of the acyclic phosphonate.

The hydrogen and carbon assignments for final products **3-8** were made based on ^{1}H and ^{13}C NMR spectra. The chemical shift values of the signals, their multiplicity, coupling constants, and integrals were considered. The ^{1}H NMR spectra of compounds **3-8** contained singlets representing the hydrogens of the 1,2,3-triazole ring between 8.06 and 8.90 ppm, which confirmed the formation of the triazole ring. In the ^{13}C NMR spectra of final products **3-8**, signals between 44.34 and 45.51 ppm from the bridging CH_2 located between the imidazole and triazole rings were observed.

To determine the purity of the synthesized compounds, high-performance liquid chromatography (HPLC) was used, the percentage total peak area represented by the product peak was determined in a scan of 190-800 nm. All final products (**3-8**) showed purities between 97% and 99.9%.

3.2. Biological evaluation

Analysis of the *in vitro* cytotoxicity to mammalian cells was based on LC_{50} values, the concentration that has a 50 % lethality to the cells. Cytotoxicities of the compounds were determined in L929 cell cultures after treatment for 96 h at 37 °C. The trypanocidal experiments performed *in vitro* were conducted using the intracellular amastigote forms of *T. cruzi* (Tulahuen strain transfected with β-galactosidase, DTU VI) and bloodstream trypomastigotes (Y strain, DTU II). The results of antiparasitic biological evaluation were expressed in terms of the half maximal effective concentration (EC_{50} values, μM). Afterwards, the therapeutic index or selectivity index (SI) was determined based on the mean values of the LC_{50}/EC_{50} ratio, which corresponds to the therapeutic window (a measure of drug safety). High values of SI indicate that there is an ample safety margin between the dose that is effective and the dose that is toxic (Table 1), and the *in vitro* prediction for a Chagas disease hit is an EC_{50} <10 μM against intracellular *T. cruzi* and a greater than 10- fold selectivity window for cytotoxicity using a mammalian cell line.[54]

The biological evaluation showed that all compounds were active *in vitro* against intracellular amastigote forms, with the exception of compound **7**. Compounds **3** and **4** are equipotent against *T. cruzi* amastigote forms showing EC_{50} values of 7.9 μM and 8.0 μM, respectively, which makes them half as active as Bnz (EC_{50} = 4 ± 1.5 μM). Compound **5** (EC_{50} = 4.4 μM) was the most promising against *T. cruzi* amastigote forms with a potency similar to Bnz. Finally, compound **8** presented an EC_{50} value of 10.9 μM against amastigote forms, which is only one-third as potent as Bnz. Therefore, from the results of Table 1, the importance of the aromatic ring attached to the 1,2,3-triazole ring could clearly be seen since **7**, which has no such substituent, was inactive. The replacement of the benzyl group with a 2-methyl-3-nitrophenyl moiety (compound **5**) increased the activity of the compound relative to the activities of other derivatives and Bnz. The most active derivatives were further tested against bloodstream trypomastigotes forms of *T. cruzi* (Y strain, DTU II) for 24 h at 37 °C (Table 1). These forms are, as the intracellular amastigotes, very relevant parasite forms for mammalians infection and must be considered in a drug cascade screening for CD.[48]

Table 1 – Results of the biological and cytotoxic evaluation of compounds **3-8** in amastigote and bloodstream trypomastigotes forms of *T. cruzi*, and their corresponding selectivity index (SI).

Compounds	**Amastigote Forms**			**Trypomastigote Forms**	
	EC_{50} (μM)	LC_{50} (μM)	SI	EC_{50} (μM)	SI
3	7.9 ± 3.3	> 200	> 25	28 ± 10	7
4	8.0 ± 4.1	> 200	> 25	3 ± 1	67
5	4.4 ± 1.7	182	42	2.2 ± 0.3	83
6	13 ± 2.8	182	14	Not determined	Not determined
7	Inactive	> 200	Not determined	Not determined	Not determined
8	10.9 ± 4.6	125	11.5	14 ± 4	9
Benznidazole	4 ± 1.5	> 200	> 50	13 ± 2	77

The *in vitro* findings against bloodstream trypomastigotes demonstrate that compounds **4**, **5**, and **8** were the most active against this non-multiplying but highly infective parasite stage. In addition, the presence of a 3-cyanophenyl group makes a compound (**4**) four times more potent than Bnz against trypomastigote forms. Interestingly, although the 1,2,3-triazole ring can be described as an amide bioisostere, in compound **3**, it was observed that this replacement reduces the biological activity by half compared to Bnz. Nevertheless, with respect to cytotoxicity, these derivatives were not toxic. Compounds **4** and **5** (Table 1) are the most promising, exhibiting EC_{50} values ≤ 3 μM, making them at least 4.3 and 5-fold, respectively, more active than the reference drug (Bnz, $EC_{50} = 13$ μM). For this reason, they were submitted to further *in vivo* analyses using murine models. Webster male mice (18-20 g) were infected by intraperitoneal (ip) injection of 10^4 bloodstream trypomastigotes (Y strain) and then submitted to one of two different therapeutic regimens: (a) two doses (the first at 5 day post infection (5 dpi) and the second dose at the 8 dpi, which correspond to the parasitaemia onset and peak using this experimental model, respectively) or (b) five consecutive doses, starting the therapy at 5 dpi.[55] Before the *in vivo* efficiency was determined, acute toxicity was evaluated as previously reported to identify the NOAEL levels.[56] Our data demonstrated that the administration of compound **4** at 5 and 8 dpi did not protect against *T. cruzi* infection as it was unable to reduce either parasitaemia levels (Figure 2A) or mortality rates (Figure 2B). The *in vivo* analysis against *T. cruzi* infection showed that compound **5** administered at 5 and 8 dpi resulted in a mild reduction in the parasite load; **5** gave a 37% reduction of the parasitaemia peak but was unable to improve animal survival rates, which reached 100% mortality, similar to those mice that were infected and only treated with the vehicle used to dilute the studied compound (Figure 2B).

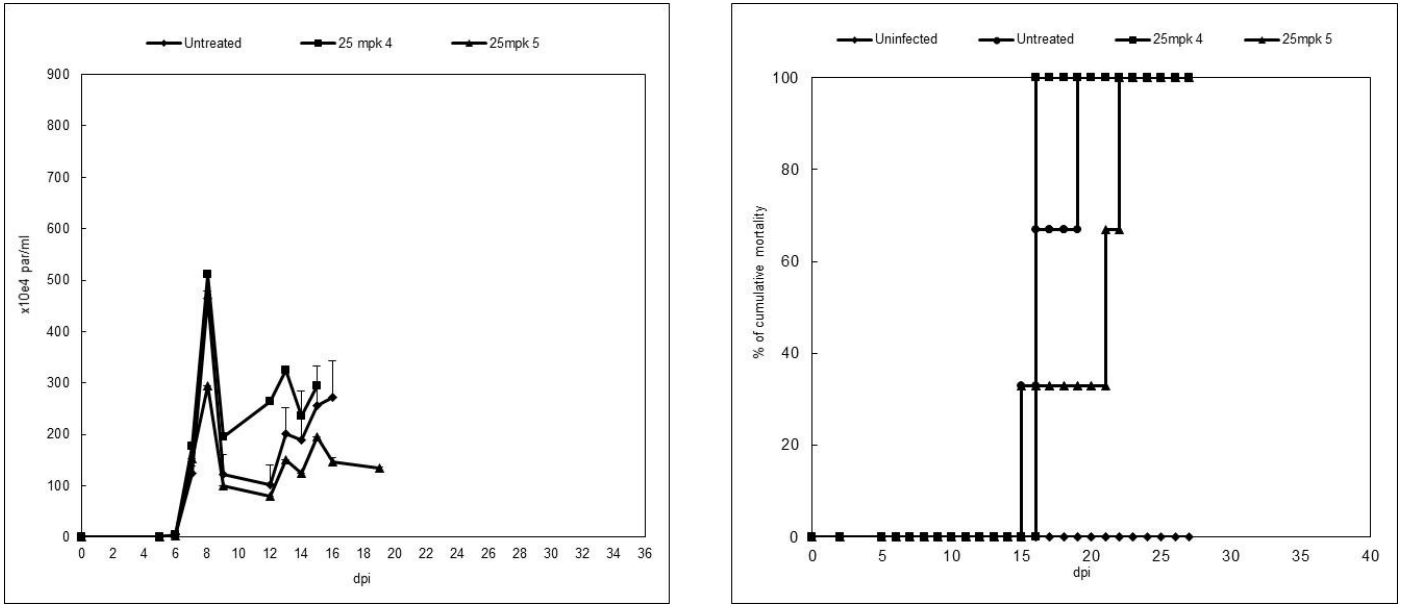

Figure 2. The activity of compounds **4** and **5** on experimental infection of Swiss male mice infected with *T. cruzi* (Y strain) and treated at the parasitaemia onset (5 dpi) and peak (8 dpi). (A) Parasitaemia levels and (B) cumulative mortality.

.

To determine if longer periods of drug exposure could improve the pharmacological distribution and disponibility, a second analysis was performed involving the daily administration of compounds **4** and **5** for consecutive days. The data showed that administration of **5** for 5 consecutive days induced a considerable reduction in the parasite load, reaching a 52% decrease in the parasitaemia peak at 8 dpi when doses of 100 mg/kg were given (Figure 3A). On the other hand, compound **4** increased the parasitaemia levels, possibly due to drug toxicity although both *in vitro* and acute toxicity studies performed using healthy animals did not reveal a toxic profile. In fact, no direct correlation does always exist between toxicity *in vitro* and *in vivo*. Although a very toxic compound *in vitro* is more prone to be toxic *in vivo*, the inverse (non-toxic *in vitro* but toxic *in vivo*) may occur due to the complex metabolic pathways and flows *in vivo* that are not present in the *in vitro* cell cultures and then, some of their resulting metabolic elements may induce animal side effect such as hepatotoxicity, cardiotoxicity, among other toxic events. As a direct comparison, as expected, using Bnz, the reference drug, resulted in complete parasitaemia suppression.[48] Regarding mortality rates, Bnz resulted in 100% animal survival, while test compound **5** only reduced mice mortality rates by a small amount, leading to 17% mice survival (Figure 3B). The untreated group and the group treated with compound **4** both exhibited 100% animal death (Figure 3B).

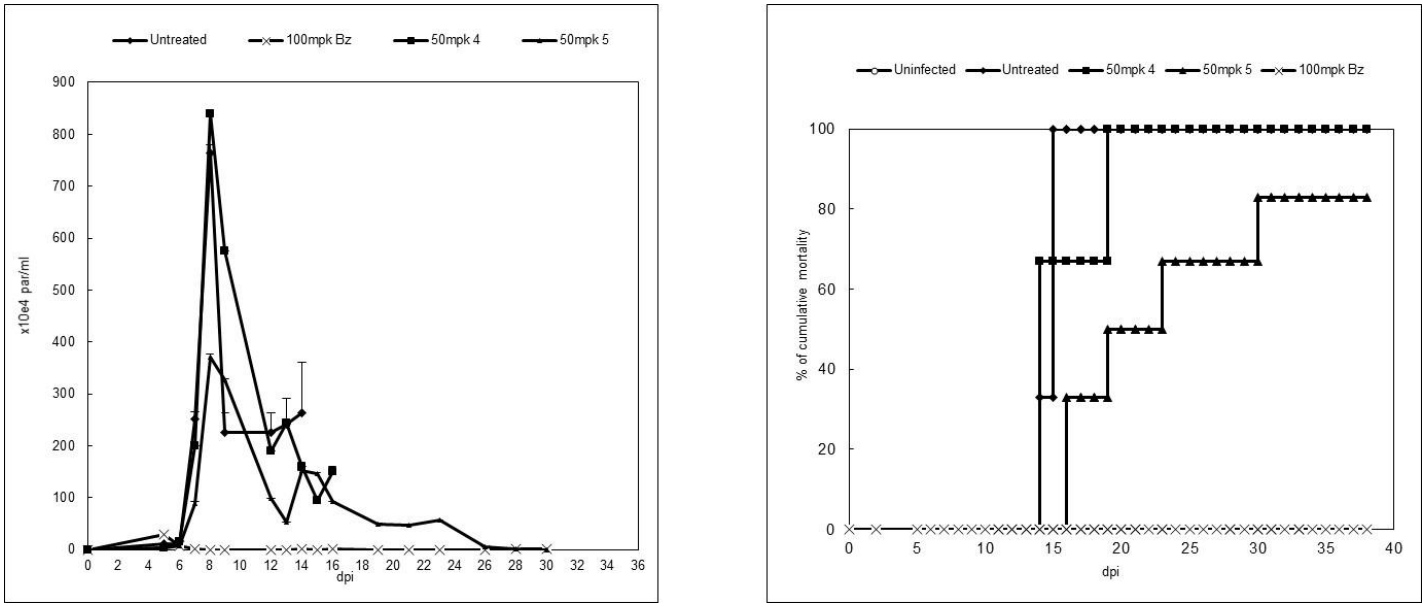

Figure 3. The activity of compounds **4** and **5** on experimental infection of Swiss male mice infected with *T. cruzi* (Y strain) and treated for five consecutive days starting at the parasitaemia onset (5 dpi). (A) Parasitaemia levels and (B) cumulative mortality.

Compound **3**, an isostere of Bnz, was assayed *in vivo* to verify the influence of the 1,2,3-triazole ring on anti-*T. cruzi* activity and mammalian cells cytotoxicity. The results showed that the non-toxic concentrations of this compound (that displayed a NOAEL > 400 mg/kg) revealed that the administration of 5 daily consecutive doses (100 mg/kg/day) induced a 25% decrease in the parasitaemia peak at 8 dpi (Figure 4A); as expected, Bnz resulted in complete parasitaemia suppression.[48] Regarding mortality rates, Bnz resulted in 100% animal survival, while compound **3** provided no improvement in mice mortality; untreated mice displayed 0% animal survival (Figure 4B). This result showed that substitution of the amide group by a 1,2,3-triazole caused a higher toxicity *in vivo*.

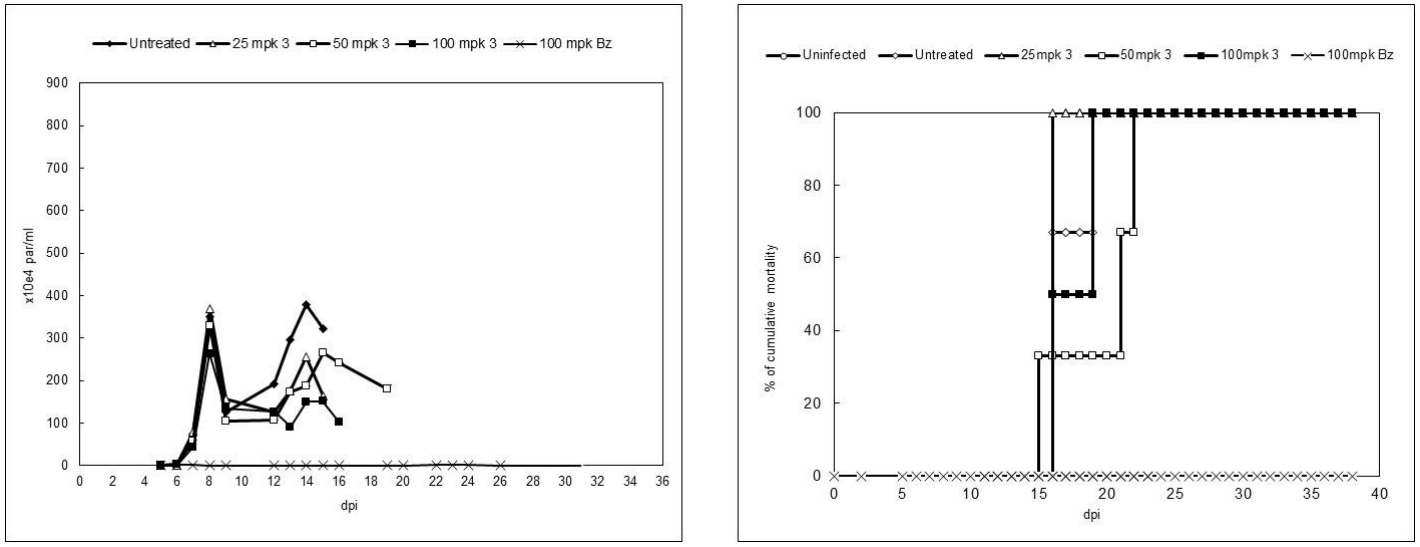

Figure 4. The activity of compound **3** on experimental infection of Swiss male mice infected with *T. cruzi* (Y strain) and treated for five consecutive days starting at the parasitaemia onset (5 dpi). (A) Parasitaemia levels and (B) cumulative mortality.

4. Conclusions

Six novel compounds, **3**-**8**, were synthesized in only a few reactions. The planned compounds containing 1,4-disubstituted 1,2,3-triazole rings were obtained using "*click chemistry*" with good yields and high purity. The biological testing *in vitro* and *in vivo* using *T. cruzi* models demonstrated that although the 1,2,3-triazole ring can be described as amide bioisostere, in compound **3**, an isostere of Bnz, this replacement reduces the biological activity to approximately half that of Bnz. Compounds **4** and **5** showed the most promising antiparasitic profiles; **5** was the most potent against both amastigotes and bloodstream trypomastigotes and was more potent than Bnz *in vitro*. Nevertheless, only **5** demonstrated *in vivo* activity, but it decreased the parasitism only 37% compared to Bnz, and it was highly toxic. In addition, even with long periods of exposure to compound **5**, only a 52% decrease in the parasitaemia peak was observed. Despite analogues **3**-**8** not showing cytotoxicity, they were very toxic *in vivo*. Therefore, these results suggest further optimization of these candidates are needed to identify new therapeutic agents that are more potent and less toxic for Chagas disease, a silent and neglected pathology that affects millions of people and lacks a feasible therapy. In addition, we hope that our active compounds share the same mechanisms of action with Bnz, owing to their structural similarity; thus, more studies must be performed.

Acknowledgements

We are grateful to FIOCRUZ, CAPES, CNPq, and FAPERJ for funding this work. MNCS is fellow of CNPq, and CNE (FAPERJ). The authors appreciate the technical help of Marcos Meuser Batista.

Conflict of Interest

All authors report no conflict of interest.

References and notes

[1] A. Biolo, A. L. Ribeiro, N. Clausell, *Prog. Cardiovasc. Dis.* **2010**, *52*, 300.

[2] F. X. Lescure, G. Le Loup, H. Freilij, M. Develoux, L. Paris, L. Brutus, et al., *Lancet Infect. Dis.* **2010**, *10*, 556.

[3] P. J. Hotez, E. Dumonteil, L. Woc-Colburn, J. A. Serpa, S. Bezek, M. S. Edwards, et al., *PLoS Negl. Trop. Dis.* **2012**, *6*, e1498.

[4] WHO | Chagas disease (American trypanosomiasis). *WHO* **2017**.

[5] S. P. Vega Royero, G. J. Sibona, *J. Theor. Biol.* **2014**, *340*, 23.

[6] S. K. Meymandi, C. J. Forsyth, J. Soverow, S. Hernandez, D. S. Hernandez, S. P. Montgomery, et al., *Clin. Infect. Dis.* **2017**, *64*, 1182.

[7] J. R. Coura, S. L. De Castro, *Mem. Inst. Oswaldo Cruz* **2002**, *97*, 3.

[8] J. D. Maya, B. K. Cassels, P. Iturriaga-Vásquez, J. Ferreira, M. Faúndez, N. Galanti, et al., *Comp. Biochem. Physiol. - A Mol. Integr. Physiol.* **2007**, *146*, 601.

[9] S. R. Wilkinson, M. C. Taylor, D. Horn, J. M. Kelly, I. Cheeseman, *Proc. Natl. Acad. Sci.* **2008**, *105*, 5022.

[10] M. A. Rajão, C. Furtado, C. L. Alves, D. G. Passos-Silva, M. B. de Moura, B. L. Schamber-Reis, et al., *Environ. Mol. Mutagen.* **2014**, *55*, 309.

[11] A. Rassi, J. A. Marin-Neto, A. Rassi, *Mem. Inst. Oswaldo Cruz* **2017**, *112*, 224.

[12] M. de N. C. Soeiro, S. L. de Castro, *Open Med. Chem. J.* **2011**, *5*, 21.

[13] B. Zingales, R. G. A. Araujo, M. Moreno, J. Franco, P. H. N. Aguiar, S. L. Nunes, et al., *Mem. Inst. Oswaldo Cruz* **2015**, *110*, 433.

[14] J. M. Holub, K. Kirshenbaum, *Chem. Soc. Rev.* **2010**, *39*, 1325.

[15] E. M. Guantai, K. Ncokazi, T. J. Egan, J. Gut, P. J. Rosenthal, P. J. Smith, et al., *Bioorganic Med. Chem.* **2010**, *18*, 8243.

[16] N. Boechat, M. D. L. G. Ferreira, L. C. S. Pinheiro, A. M. L. Jesus, M. M. M. Leite, C. C. S. Júnior, et al., *Chem. Biol. Drug Des.* **2014**, *84*, 325.

[17] F. MAC Barreiro EJ, *Eliezer J. Barreiro - Química Medicinal - As Bases Moleculares Da Ação Dos Fármacos, 2ª Edição.pdf*, Barreiro EJ, F. MAC, Ed., 3ª., Artmed, Porto Alegre, 2015.

[18] M. C. Fernandes, E. N. Da Silva, A. V. Pinto, S. L. De Castro, R. F. S. Menna-Barreto, *Parasitology* **2012**, *139*, 26.

[19] P. H. F. Stroppa, L. M. R. Antinarelli, A. M. L. Carmo, J. Gameiro, E. S. Coimbra, D. Adilson, *Bioorg. Med. Chem.* **2017**, *25*, 3034.

[20] H. N. Nagesh, N. Suresh, G. V. S. B. Prakash, S. Gupta, J. V. Rao, K. V. G. C. Sekhar, *Med. Chem. Res.* **2015**, *24*, 523.

[21] K. Rajavelu, M. Subaraja, P. Rajakumar, *New J. Chem.* **2018**, *42*, 3282.

[22] M. De Lourdes G. Ferreira, L. C. S. Pinheiro, O. A. Santos-Filho, M. D. S. Peçanha, C. Q. Sacramento, V. Machado, et al., *Med. Chem. Res.* **2014**, *23*, 1501.

[23] M. N. Noolvi, R. Karpoormath, *Eur. J. Med. Chem.* **2018**, *5*, 137.

[24] N. Boechat, V. F. Ferreira, S. B. Ferreira, M. D. L. G. Ferreira, F. D. C. Da Silva, M. M. Bastos, et al., *J. Med. Chem.* **2011**, *54*, 5988.

[25] K. Lal, P. Yadav, A. Kumar, A. Kumar, A. K. Paul, *Bioorg. Chem.* **2018**, *77*, 236.

[26] Y. Hu, S. Zhang, F. Zhao, C. Gao, L. Feng, *Eur. J. Med. Chem.* **2017**, *133*, 255.

[27] H. G. Bonacorso, M. C. Moraes, F. M. Luz, P. S. Quintana, N. Zanatta, M. A. P. Martins, *Tetrahedron Lett.* **2015**, *56*, 441.

[28] S. Ferreira, A. C. R. Sodero, M. F. C. Cardoso, E. S. Lima, C. R. Kaiser, F. P. Silva, et al., *J. Med. Chem.* **2010**, *53*, 2364.

[29] M. Mohammadi-Khanaposhtani, M. Saeedi, N. S. Zafarghandi, M. Mahdavi, R. Sabourian, E. K. Razkenari, et al., *Eur. J. Med. Chem.* **2015**, *92*, 799.

[30] R. Suzuki, D. Nozawa, A. Futamura, R. Nishikawa-Shimono, M. Abe, N. Hattori, et al., *Bioorg. Med. Chem.* **2015**, *23*, 1260.

[31] Y. C. Li, C. Qi, S. H. Li, H. J. Zhang, C. H. Sun, Y. Z. Yu, et al., *J. Am. Chem. Soc.* **2010**, *132*, 12172.

[32] S. Satapathi, A. Bheemaraju, S. K. Surampudi, D. Venkataraman, J. Kumar, *IEEE Sens. J.* **2014**, *14*, 4334.

[33] Y. Jin, H. Zhao, H. Lu, C. Kuemmel, J. Zhang, D. Wang, *Molecules* **2015**, *20*, 1088.

[34] P. Thirumurugan, D. Matosiuk, K. Jozwiak, *Chem. Rev.* **2013**, *113*, 4905.

[35] P. De Andrade, O. A. Galo, M. R. Carvalho, C. D. Lopes, Z. A. Carneiro, R. Sesti-costa, et al., *Bioorg. Med. Chem.* **2015**, *23*, 6815.

[36] A. Proteau-Gagné, K. Rochon, M. Roy, P.-J. Albert, B. Guérin, L. Gendron, et al., *Bioorg. Med. Chem. Lett.* **2013**, *23*, 5267.

[37] Y. L. Angell, K. Burgess, *Chem. Soc. Rev.* **2007**, *36*, 1674.

[38] J. A. Urbina, R. Docampo, *Trends Parasitol.* **2003**, *19*, 495.

[39] J. A. Urbina, *Acta Trop.* **2010**, *115*, 55.

[40] M. V Papadopoulou, B. B. Trunz, W. D. Bloomer, C. McKenzie, S. R. Wilkinson, C. Prasittichai, et al., *J. Med. Chem.* **2011**, *54*, 8214.

[41] R. Bejot, L. Carroll, K. Bhakoo, J. Declerck, V. Gouverneur, *Bioorganic Med. Chem.* **2012**, *20*, 324.

[42] S. Yap, O. L. Woodman, P. J. Crack, S. J. Williams, *Bioorganic Med. Chem. Lett.* **2011**, *21*, 5102.

[43] Y. Joyard, L. Bischoff, V. Levacher, C. Papamicael, P. Vera, P. Bohn, *Lett. Org. Chem.* **2014**, *11*, 208.

[44] S. G. Alvarez, M. T. Alvarez, *Synthesis (Stuttg).* **1997**, *1997*, 413.

[45] I. E. Głowacka, J. Balzarini, A. E. Wrõblewski, *Arch. Pharm. (Weinheim).* **2013**, *346*, 677.

[46] K.-C. Tiew, D. Dou, T. Teramoto, H. Lai, K. R. Alliston, G. H. Lushington, et al., *Bioorg. Med. Chem.* **2012**, *20*, 1213.

[47] B. G. M. Youssif, K. Okuda, T. Kadonosono, O. I. A. R. Salem, A. A. M. Hayallah, M. A. Hussein, et al., *Chem. Pharm. Bull.* **2012**, *60*, 402.

[48] A. J. Romanha, S. L. de Castro, M. de N. C. Soeiro, J. Lannes-Vieira, I. Ribeiro, A. Talvani, et al., *Mem. Inst. Oswaldo Cruz* **2010**, *105*, 233.

[49] B. Timm, P. da Silva, M. Batista, F. da Silva, C. da Silva, R. Tidwell, et al., *Antimicrob Agents Chemother.* **2014**, *58*, 3720.

[50] D. da G. J. Batista, M. M. Batista, G. M. de Oliveira, P. B. do Amaral, J. Lannes-Vieira, C. C. Britto, et al., *Antimicrob. Agents Chemother.* **2010**, *54*, 2940.

[51] J. S. De Araújo, C. F. Da Silva, D. G. J. Batista, P. B. Da Silva, M. B. Meuser, C. A. F. Aiub, et al., *Antimicrob. Agents Chemother.* **2014**, *58*, 4191.

[52] E. B. T. Diogo, G. G. Dias, B. L. Rodrigues, T. T. Guimarães, W. O. Valença, C. A. Camara, et al., *Bioorganic Med. Chem.* **2013**, *21*, 6337.

[53] S. B. Ferreira, M. S. Costa, N. Boechat, R. J. S. Bezerra, M. S. Genestra, M. M. Canto-Cavalheiro, et al., *Eur. J. Med. Chem.* **2007**, *42*, 1388.

[54] K. Katsuno, J. N. Burrows, K. Duncan, R. H. Van Huijsduijnen, T. Kaneko, K. Kita, et al., *Nat. Rev. Drug Discov.* **2015**, *14*, 751.

[55] F. H. Guedes-Da-Silva, D. G. J. Batista, C. F. Da Silva, M. B. Meuser, M. R. Simões-Silva, J. S. De Araújo, et al., *Antimicrob. Agents Chemother.* **2015**, *59*, 7564.

[56] F. H. Guedes-da-Silva, D. G. J. Batista, C. F. Da Silva, J. S. De Araújo, B. P. Pavão, M. R. Simões-Silva, et al., *Antimicrob. Agents Chemother.* **2017**, *61*, e02098.

Legends of Figures and Schemes

Figure 1. Chemical structures of benznidazole (**1**, Bnz) and nifurtimox (**2**), which are used in the treatment of Chagas disease.

Figure 2. The activity of compounds **4** and **5** on experimental infection of Swiss male mice infected with *T. cruzi* (Y strain) and treated at the parasitaemia onset (5 dpi) and peak (8 dpi). (A) Parasitaemia levels and (B) cumulative mortality.

Figure 3. The activity of compounds **4** and **5** on experimental infection of Swiss male mice infected with *T. cruzi* (Y strain) and treated for five consecutive days starting at the parasitaemia onset (5 dpi). (A) Parasitaemia levels and (B) cumulative mortality.

Figure 4. The activity of compound **3** on experimental infection of Swiss male mice infected with *T. cruzi* (Y strain) and treated for five consecutive days starting at the parasitaemia onset (5 dpi). (A) Parasitaemia levels and (B) cumulative mortality.

Scheme 1. Design of new derivatives **3-8**.

Scheme 2. Synthetic methodology for the preparation of final products **3-8**.

Supplementary Material

Supplementary material that may be helpful in the review process should be prepared and provided as a separate electronic file. That file can then be transformed into PDF format and submitted along with the manuscript and graphic files to the appropriate editorial office.